Marine Vehicle Path Following Using Inner-Outer Loop Control

P. Maurya [*,**], **A. Pedro Aguiar** [**], **A. Pascoal** [**]

[*] *National Institute of Oceanography, Marine Instrumentation Division Dona Paula Goa-403004, India (E-mail: maurya@nio.org)*
[**] *Instituto Superior Tecnico - Institute for Systems and Robotics (IST-ISR) Lisbon 1049-001, Portugal (E-mail: antonio@isr.ist.utl.pt)*

Abstract: This paper addresses the problem of marine vehicle path following using inner-outer loop control, with due account for the vehicle dynamics. We propose an inner-outer control structure that lends itself to a simple intuitive interpretation and exhibits three key advantages: i) it allows for decoupling in the design of the inner and outer control loops, ii) the design of the outer loop controller does not require in depth knowledge of the internal vehicle dynamics, and iii) it affords practitioners a very convenient method to effectively implement path following controllers on a wide range of vehicles. The mathematical tools used for systems characterization and stability analysis borrow from Input to Output Stability (IOS) theory and small gain theorems. In this paper, formal system analysis is done only for the case where the paths to be followed are straight lines. However, the technical machinery developed and the results obtained shed light into the process of designing path following controllers with an inner-outer loop structure for arbitrary paths. The efficacy of the path following control structure developed has been proven during tests with an AUV and an ASV at sea.

Keywords: Path following, Inner-outer loop control, Input to Output Stability, AUVs, ASVs

1. INTRODUCTION

In many oceanographic missions of interest, marine vehicles are required to follow spatial paths accurately. An example is the case where an autonomous underwater vehicle (AUV) executes a lawn-mowing manoeuvre along a desired path, at a speed that may be a function of its position along the path. In this case, no strict temporal constraints are imposed on the motion of the vehicle. This is in striking contrast with trajectory tracking, where the reference for the vehicle motion is given explicitly in terms of "space versus time" coordinates. This strategy is seldom pursued in practice, for it may lead to situations where, by requesting that a vehicle track a desired inertial trajectory, the required speed with respect to the water may either be too small (leading to the loss of surface control authority) or too high (exceeding the capability of the propulsion systems installed on board). Path following control systems overcome these problems and, if properly designed, lead naturally to vehicle trajectories that are smoother than those obtained with trajectory tracking control. See for example Micaelli and Samson (1993), Encarnacao and Pascoal (2000), Silvestre (2000), Fossen (2002), Aguiar et al. (2005) and the references therein for a discussion of this circle of ideas.

Interestingly enough, path following is at the core of a number of methods used for multiple vehicle cooperative control along a set of fixed spatial paths, while holding a desired formation pattern. See for example Pascoal et al. (2006) and Ghabchello et al. (2009) for an introduction to this subject. In this set-up, each vehicle executes a path following maneuver along its assigned path; a decentralized control law adjusts the different vehicle speeds so that the desired geometrical pattern (compatible with the paths) is achieved. The above comments add weight to the fact that there is a need for the development of methods for reliable path following that can be implemented on heterogeneous vehicles even when detailed knowledge of their dynamics is not available.

The literature on path following is extensive and the types of control laws available display a vast choice of techniques that borrow from linear and nonlinear control theory. Representative examples can be found in Breivik and Fossen (2005), Park et al. (2007), Vanni (2007), Aguiar and Hespanha (2007), and Indiveri and Zizzari (2008). Path following has also been addressed extensively in the aircraft control field, where inner-outer (dynamic-kinematic) loop control structures are pervasive and have shown to be effective. In particular, inner-outer loop control structures exhibit a fast-slow temporal scale separation that yields simple "rules of thumb" for controller tuning. Stated intuitively , the inner loop dynamics should be much faster than those of the outer loop. This qualitative result is well rooted in singular perturbation theory Khalil (2001). Conceptually, the procedure described has three key advantages: i) it decouples the design of the inner and outer control loops, ii) the structure of the outer loop controller does not depend on the dynamics of the vehicle, and iii) it affords practitioners a very convenient method to effectively implement path following controllers on a wide range of vehicles.

With the set-up adopted, the outer kinematic loop is designed separately by assuming that its output variables can be tracked infinitely fast by the inner dynamic loop. In practice, this does not hold true. Furthermore, many vehicle suppliers equip their platforms with inner dynamic control loops for which only a general characterization of the resulting plant-controller dynamics is available. It is therefore required that the system designer tune the outer loop control based on the characteristics of the inner loop, so that the resulting combination yields a stable system with good performance. In some cases, tuning of the inner loop may also be required. To do this, however requires going well beyond qualitative statements regarding fast-

slow temporal scale separation and to actually analyze the inner-outer loop combination to obtain quantitative relationships aimed at assessing stability and performance. Furthermore, to be of practical value the analysis must take into account the fact that the inner loops dynamics are often described in very general terms. For example, in the case of linear systems the end user may only know the approximate bandwidth and static gain of the inner loop control system. In the general nonlinear case, some form of Input to State Stability (ISS) or Input to Output Stability (IOS) characterizations may be available, see Khalil (2001).

Motivated by the above considerations, this paper addresses the problem of path following for marine vehicles by resorting to inner-outer control loops, with due account for the vehicle dynamics and currents. The tools adopted borrow from nonlinear control theory, whereby the cascade and feedback systems of interest are characterized in terms of their IOS properties. To derive quantitative relationships for proper controller tuning an IOS small-gain theorem is used. The analysis applies to a very general class of vehicles. In this paper, formal system analysis is done only for the case where the paths to be followed are straight lines. However, the technical machinery developed and the results obtained shed light into the process of designing path following controllers with an inner-outer loop structure for arbitrary paths.

For the sake of simplicity, the paper addresses the case where the vehicles under consideration move in 2D space. In this case, the path following controller is designed as the combination of a kinematic outer-loop that issues heading commands to an inner loop consisting of the feedback combination of the vehicle itself and a heading controller (heading autopilot). The speed of the vehicle may be kept approximately constant by a dedicated controller that is not analyzed here. *The basic assumptions are that the plant / inner loop controller interconnection is characterized in very general terms by an IOS-like relationship, and no in depth knowledge of the internal vehicle dynamics is available.* This is of crucial importance to seamlessly implement path following controllers on vehicles that come equipped with heading autopilots.

Due to space limitations, and for the sake of clarity, we have chosen to focus on showing stability of the complete path following control system. A proof of convergence that relies on ISS system characterization is available in Maurya et al. (2009). Notice also that the present paper includes only an indication of the proofs of the main theoretical results required for path following controller design. Full details are available in Maurya et al. (2009).

The paper is organized as follows. Section 2 formulates the problem of path following for straight lines in 2D, proposes an inner-outer loop control structure for its solution, and gives an indication of the proof of stability of the resulting feedback control system. Section 3 describes the results of simulations and field test results with an ASV. Finally, Section 4 contains the main conclusions and discusses problems that warrant further research.

2. PATH FOLLOWING ALGORITHM IN 2D

The path following problem that we consider in the paper can be simply explained by referring to fig.1. In the figure, $\{I\} = \{x_I, y_I\}$ and $\{B\} = \{x_B, y_B\}$ denote an inertial frame and a body-frame that is solidary with the vehicle, respectively. Variable V_w is the velocity of the vehicle with respect to the water expressed in $\{B\}$, V_c is the velocity of the current in $\{I\}$, and V is the total inertial

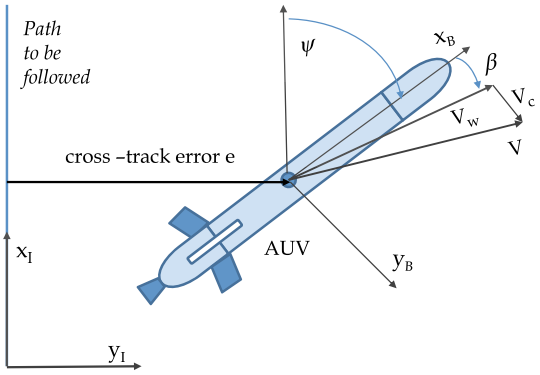

Fig. 1. Cross track error for straight line following

velocity, also expressed in $\{I\}$. As is customary, ψ and β denote yaw and sideslip angles, respectively. For motion in the horizontal plane, the vehicle is equipped with a stern propeller and two coupled vertical stern planes. The total speed of the vehicle is set by "freezing" the speed of rotation of the stern propeller. The stern rudders are then used in common mode to control the vehicle's heading. Let P denote the position of the center of mass of the AUV, expressed in $\{I\}$. Clearly, $\dot{P} = R(\psi)V_w + V_c$ where $R(.)$ denotes the rotation matrix from $\{B\}$ to $\{I\}$, parameterized by ψ. Equivalently, $\dot{P} = R(\psi + \beta)[\|V_w\| \ 0]^T + V_c$, where β is angle of side slip. It follows from the above that the evolution of the distance from the center of mass of the AUV to the path, usually called cross track error and denoted e, satisfies $\dot{e} = \sin(\psi + \beta)\|V_w\| + v_{cy}$, where v_{cy} denotes the component of V_c along the unit vector y_I. Assume for simplicity of exposition that the total speed $\|V_w\|$ is held constant and equal to $U > 0$. This assumption can be lifted and the results extended to the case where $\|V_w\| > \|V_c\|$. The objective (path following problem) is to steer the vehicle using the stern planes so that e will converge to zero. In what follows, this is done by adopting a two step procedure: first, assuming that the heading angle can be commanded instantaneously, design a kinematic outer-loop with heading as a command variable (virtual control) so that the cross track error converges to zero; then, use a dynamic inner-loop loop (heading controller) so that the actual heading angle track the commanded angle. It is tacitly assumed that the heading control loop (autopilot) is characterized in very general terms via an IOS relationship. Conditions are determined and tuning rules are offered under which the complete path following system is stable. See Maurya et al. (2009) for a convergence result.

Path Following Algorithm: the Rationale

The rationale for the control law derived can be best understood by considering the simplified case where the sideslip angle is zero (this assumption is lifted afterwards). In this situation,

$$\dot{e} = U\sin(\psi) + v_{cy} \tag{1}$$

which, in the absence of the term v_{cy}, can be re-written as

$$\dot{e} = Uu,$$

with $u = \sin(\psi)$. We now make the trivial and yet crucial observation: should we be free to manipulate the variable u, then the choice of control law $u = -(K_1/U)e$ would yield asymptotic exponential convergence of e to the origin. To further push this line of thought, notice also that the existence of the fixed bias v_{cy} motivates the

introduction of an integral term in the virtual input u, which is now re-rewritten as

$$u = -\frac{1}{U}\left(K_1 e - K_2 \int_0^t e(\tau)\, d\tau\right).$$

As a consequence, the dynamics of e become

$$\dot{e} + K_1 e + K_2 \int_0^t e(\tau)\, d\tau = 0$$

Let

$$\varsigma = \int_0^t e(\tau)\, d\tau.$$

Then,

$$\ddot{\varsigma} + K_1 \dot{\varsigma} + K_2 \varsigma = 0$$

The above system is second order system and the gains K_1 and K_2 can now be chosen so as to obtain a desired natural frequency and damping factor. Clearly, the above virtual control suggests that the desired command for heading be written as

$$\psi_d = \sin^{-1}(sat(u)),$$

abbreviated $\psi_d = \sin^{-1} u_s$, with $u_s = sat(u)$, where

$$sat(u) = \begin{cases} u & if\ |u| < l_s \\ l_s & if\ u \geqslant l_s, \\ -l_s & if\ u \leqslant -l_s \end{cases}$$

$0 < l_s < 1$, and the saturation function is introduced to guarantee that the argument of $sin^{-1}(.)$ lies in the interval $[-1, +1]$. In what follows, it is important to introduce an antiwindup mechanism in the integral term of u. For this reason, the final form of the control law for ψ_d involves a new definition of u and is given in terms of the operator $f : e \to \psi_d$ defined by

$$\psi_d = \sin^{-1}(sat(u)); u = \left(-\frac{K_1 e}{U} - \frac{K_2}{U}\varsigma\right)$$

where ς is the output of the dynamical system $f_{aw}(e) : e \to \varsigma$ with realization

$$\dot{\varsigma} = \begin{cases} e & if\ |u| < l_s \\ 0 & otherwise \end{cases} \tag{2}$$

It is possible to show, using Lyapunov-based analysis tools, that the above nonlinear control law yields convergence of the cross track error to zero if the actual vehicle heading equals the desired heading reference ψ_d. The key goal of this paper is to show that "identical behaviour" is obtained when the dynamics of the heading autopilot (inner loop) and the sideslip of the vehicle are taken into account. In particular, we show that *the basic structure and the simplicity of the outer-loop control law are preserved*. The theoretical machinery used to prove stability borrows from IOS concepts and a related small gain theorem. See Khalil (2001) for a fast paced introduction to the subject and Panteley and Ortega (1997) and Vanni (2007) for interesting applications of control techniques that bear affinity with with inner outer loop control structures. Here, we indicate briefly how the existence of the heading autopilot is taken into account without having to change the structure of the outer-loop described before.The resulting control scheme is depicted in Fig. 2, where the heading autopilot plays the role of an inner loop.

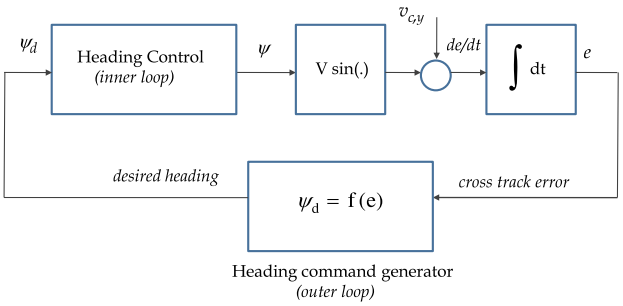

Fig. 2. Path following using inner-outer loop control

Inner Loop Dynamics

This section addresses explicitly the inclusion of the inner loop dynamics, thus lifting the assumption that the actual heading ψ equals the desired heading ψ_d. However, the dynamics of the vehicle are still simplified in that the angle of sideslip is not taken into account. This assumption will be lifted in the last part of the paper. Let

$$\tilde{\psi} = \psi - \psi_d$$

be the mismatch between actual and desired heading angles. We assume that the autopilot characteristics can be described in very general terms as an IOS (input-output-stable) system, see Khalil (2001). In order to understand the rationale for this characterization, notice that if the inner-loop dynamics are linear with static gain equal to 1, then its dynamics admit a realization of the form

$$\begin{aligned} \dot{x} &= Ax + B\psi_d \\ \psi &= Cx \end{aligned}$$

with $-CA^{-1}B = 1$. In this case, the coordinate transformation $\eta = x - A^{-1}B\psi_d$ yields the realization

$$\begin{aligned} \dot{\eta} &= A\eta + A^{-1}B\dot{\psi}_d \\ \tilde{\psi} &= C\eta \end{aligned}$$

for the operator from $\dot{\psi}$ to $\tilde{\psi}$ that characterizes the inner loop dynamics. An IOS characterization of the loop can be easily derived from the above system matrices [Khalil (2001)]. Notice, however that this type of description applies also to general nonlinear systems of the form

$$\begin{aligned} \dot{\eta} &= g(\eta, \dot{\psi}_d) \\ \tilde{\psi} &= h(\eta, \dot{\psi}_d) \end{aligned}$$

and allows for a somewhat loose, yet quantifiable description of the inner-loop dynamics. This justifies the IOS characterization of the inner loop dynamics as

$$\left\|\tilde{\psi}(t)\right\| \leq \beta_f\left(\left\|\eta(0)\right\|, t\right) + \gamma_f\left(\sup_{t_0 \leq \tau \leq t}\left\|\dot{\psi}_d(\tau)\right\|\right), \tag{3}$$

where β_f is a class $\mathcal{KL}$ function, and γ_f is a class $\mathcal{K}$ function.

The above assumption captures in a rigorous mathematical framework simple physical facts about the inner loop control system. Namely, i)if the time-derivative of the heading reference ψ_d is bounded, then the heading tracking error is bounded and ii) the dynamics of the inner loop system can be characterized in terms of bandwidth-like characteristics that are reflected in β_f and γ_f, see Khalil (2001). A simple exercise with a first order system will convince the reader that as the bandwidth of the system increases, γ_f will decrease. For practical purposes, the latter can be viewed as a "tuning knob" during the path following controller design phase. For analysis purposes,

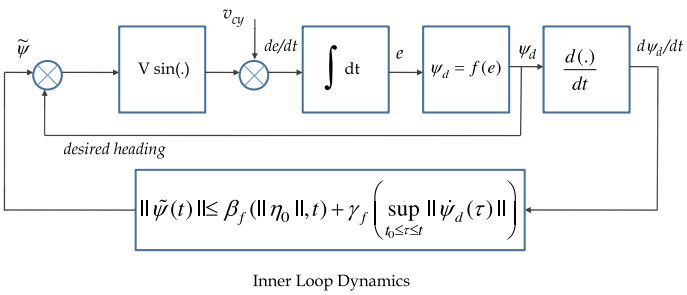

Fig. 3. Inner-outer loop control: an IO characterization

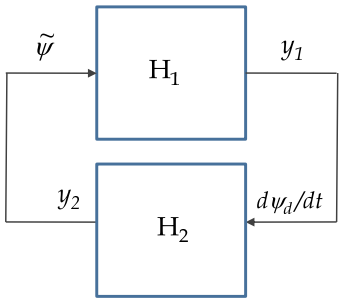

Fig. 4. General feedback interconnection

it is also required to ensure that not only $\tilde{\psi}$ but also the remaining variables in the inner loop be bounded in response to $\dot{\psi}_d$. This fact can be easily captured with an ISS condition of the type

$$\|\eta(t)\| \leq \beta_g\left(\|\eta(0)\|, t\right) + \gamma_g\left(\sup_{t_0\leq\tau\leq t}\left\|\dot{\psi}_d(\tau)\right\|\right), \qquad (4)$$

for some $\beta_g \in \mathcal{KL}$ and $\gamma_g \in \mathcal{K}$. We assume such a condition holds.

At this point we make the key observation that the complete path following control system can be represented as the interconnected structure depicted in Fig. 3. The latter can be further abstracted to the scheme in Fig.4 consisting of blocks $H_1 : \tilde{\psi} \to \dot{\psi}_d$ and $H_2 : \dot{\psi}_d \to \tilde{\psi}$, a description of which is given next. To this effect, we start by defining the variable

$$\tilde{\varsigma} = K - \int_0^t e\, d\tau,$$

where K is a constant to be defined. Clearly, system H_1 admits the representation

$$\begin{aligned}
\dot{e} &= U sin(\tilde{\psi} + \psi_d) + v_{cy},\\
\dot{\tilde{\varsigma}} &= -e,\\
\psi_d &= sin^{-1}\left\{sat\left(-\frac{K_1 e}{U} + \frac{K_2\tilde{\varsigma}}{U} - \frac{KK_2}{U}\right)\right\},\\
y_1 &= \dot{\psi}_d,
\end{aligned}$$

and H_2 satisfies the IOS stability condition in (3). In what follows we show, using a small gain theorem, that the above interconnected system is closed-loop stable and all signals are bounded. Central to the proof of stability is the fact that system H_1 is IOS in the unsaturated region of operation defined by $|u| < l_s$. We purposely avoid discussing the issues that arise when the overall system enters one of the saturated regions of operation. Namely, that it will again enter the unsaturated region of operation in finite time as shown in Maurya et al. (2009).

The proof that H_1 is IOS hinges on the facts that H_1 is the composition of two auxiliary systems $H_{a1} : \tilde{\psi} \to e$ and $H_{a2} : e \to \dot{\psi}$ and that both are IOS. An indication of the proof is given next.

Consider the Lyapunov function $V(e,\tilde{\varsigma}) = \frac{1}{2}e^2 + K_2\frac{1}{2}\tilde{\varsigma}^2$ and assume that

$$\left|\tilde{\psi}\right| \leq \alpha < \pi/2$$

for all $t \geq 0$ (conditions under which this holds are described in Maurya et al. (2009). Further let $K = \frac{v_{cy}}{K_2}$. Simple but lengthy computations show that

$$\begin{aligned}
\dot{V}(e,\tilde{\varsigma}) \leq & -K_1 e^2\cos(\tilde{\psi})\\
& + |e|\left[K_2\left|\left(\cos(\tilde{\psi})-1\right)\right||\tilde{\varsigma}| + |v_{cy}|\left|\left(\cos(\tilde{\psi})-1\right)\right|\right.\\
& \left. + |U|\left|\sin(\tilde{\psi})\right|\right].
\end{aligned}$$

Using (2), it follows that $\left|\int_0^t e\, d\tau\right| < \frac{Ue_s}{K_2}$ for all t and therefore

$$|\tilde{\varsigma}| \leq \left|K + \frac{Ue_s}{K_2}\right| = \frac{1}{K_2}\left|v_{cy} + Ue_s\right|.$$

As a consequence,

$$\begin{aligned}
\dot{V}(e,\tilde{\varsigma}) \leq & -K_1 e^2\cos(\tilde{\psi})\\
& + |e|\left[C\left|\left(\cos(\tilde{\psi})-1\right)\right| + |U|\left|\sin(\tilde{\psi})\right|\right] \leq 0\\
\forall\ |e| > & \frac{|U|}{K_1\cos\alpha}\left[\frac{C}{|U|}\left|\left(\cos(\tilde{\psi})-1\right)\right| + \left|\sin(\tilde{\psi})\right|\right],
\end{aligned}$$

where $C = |v_{cy} + Ue_s| + |v_{cy}|$. It follows from standard arguments in Khalil (2001) that the cross track error e satisfies the IOS condition

$$\|e(t)\| \leq \beta_e(\nu(0), t) + \gamma_e\left(\sup_{0\leq\tau\leqslant t}\left\|\tilde{\psi}(\tau)\right\|\right)\ \ \forall\, t \geq 0, \quad (5)$$

where $\nu = (e,\tilde{\varsigma})$, β_e is a class $\mathcal{KL}$ function, and γ_e is a class $\mathcal{K}_\infty$ function given by

$$\gamma_e(r) = \left(\frac{C + |U|}{K_1\cos\alpha}\right) r.$$

From (5),

$$\|e\|_\infty \leq \beta_c + \gamma_e\left\|\tilde{\psi}\right\|_\infty, \qquad (6)$$

where $\beta_c = \beta_c(\nu(0))$ depends on the initial state but is otherwise constant in time, thus proving that H_{a1} is IOS. To show that H_{a2} is IOS start by computing $\dot{\psi}_d$ to obtain

$$\dot{\psi}_d = -\left(\frac{K_1\dot{e}}{U} + \frac{K_2 e}{U}\right)\left(1-u^2\right)^{-\frac{1}{2}}, \qquad (7)$$

where

$$\left(1-u^2\right)^{-\frac{1}{2}} \leq \eta, \qquad (8)$$

with $\eta = \frac{1}{(1-l_s^2)^{\frac{1}{2}}}$. Using equations (7) and (8) yields

$$\left\|\dot{\psi}_d\right\|_\infty \leq \frac{K_1\eta}{|U|}\|\dot{e}\|_\infty + \frac{K_2\eta}{|U|}\|e\|_\infty.$$

Furthermore, from equation (1)

$$\|\dot{e}\|_\infty \leq |U| + |v_{cy}|$$

and therefore

$$\left\|\dot{\psi}_d\right\|_\infty \leq \frac{K_1\eta}{|U|}\left(|U| + |v_{cy}|\right) + \frac{K_2\eta}{|U|}\|e\|_\infty, \qquad (9)$$

thus proving the result.

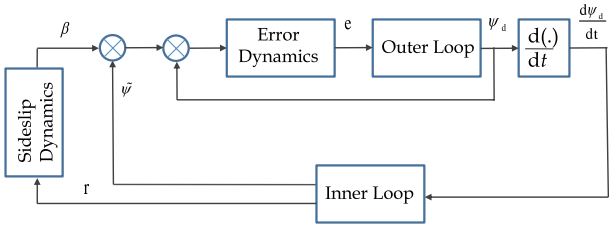

Fig. 5. Block diagram for interconnected system including side slip dynamics

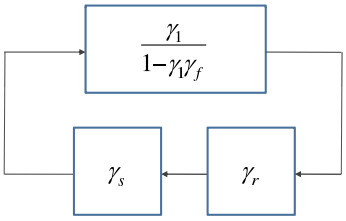

Fig. 6. Block diagram for interconnected system showing IO gains

Equipped with the above two results, it now follows from (6) and (9) that H_1 is IOS because

$$\left\|\dot{\psi}_d\right\|_\infty \leq \beta_1 + \gamma_1 \left\|\tilde{\psi}\right\|_\infty$$

where $\gamma_1 = \frac{K_2\eta}{|U|}\ \gamma_e$ and $\beta_1 = \frac{K_1\eta}{|U|}\left(|U| + |v_{cy}|\right) + \frac{K_2\eta}{|U|}\beta_c$, with γ_1 showing explicit dependence on K_1, K_2. In conclusion, the systems H_1 and H_2 are both IOS. It can now be shown, using the small gain theorem in (Khalil (2001), that the interconnected system is stable if $\gamma_1\gamma_f < 1$. This result yields a rule for the choice of gains K_1, K_2 (as functions of the inner-loop dynamic parameters) so that stability is obtained.

Sideslip Dynamics

So far, stability of the path following system has been proven by ignoring the presence of vehicle sideslip β. In this section we overcome this artificial constraint and show that stability of the closed loop system can be maintained even when the sideslip dynamics are taken into account. Again, only an indication of the proof is given for the unsaturated region. The technique that we exploit to prove stability can be best understood by referring to Figure 5, where the dynamics of β are driven by yaw rate r, an internal state of the inner loop. Let

$$\tilde{\psi} = \psi_d + \tilde{\psi}',$$

with

$$\tilde{\psi}' = \tilde{\psi} + \beta.$$

From (4), it can be concluded that the system with input $\dot{\psi}_d$ and output r is IOS and satisfies

$$\|r\|_\infty \leq \gamma_r \left\|\dot{\psi}_d\right\|_\infty + \beta_r. \tag{10}$$

We also make the assumption that the sideslip dynamical system with input r and output β is IOS and satisfies

$$\|\beta\|_\infty \leq \gamma_s \|r\|_\infty + \beta_s \tag{11}$$

for some γ_s and β_s. This assumption is valid for under-actuated open loop stable vehicles. Simple computations that build on the stability result obtained with $\beta = 0$ show that

$$\left\|\dot{\psi}_d\right\|_\infty \leq \frac{\gamma_1}{1-\gamma_1\gamma_f}\|\beta\|_\infty + \frac{1}{1-\gamma_1\gamma_f}\left(\gamma_1\beta_f + \beta_1\right), \tag{12}$$

where $\gamma_1\gamma_f < 1$. It now follows from (10) and (11) that

$$\|\beta\|_\infty \leq \gamma_s\gamma_r \left\|\dot{\psi}_d\right\|_\infty + \gamma_s\beta_r + \beta_s. \tag{13}$$

The systems characterized by the IOS relationships (12) and (13) are interconnected in feedback form as shown in Fig. 6, where only the corresponding IO gains are indicated. Again, using a small gain theorem argument it follows that the closed loop feedback system is stable if

$$\frac{\gamma_1\gamma_s\gamma_r}{1-\gamma_1\gamma_f} < 1.$$

3. IMPLEMENTATION AND FIELD TEST RESULTS

The algorithm for path following described was implemented and fully tested with success in two vehicles: the $MAYA$ AUV and the $DELFIM_x$ ASV. The first is an autonomous underwater vehicle developed at the National Institute of Oceanography, Goa, India. The latter is an autonomous surface vehicle that is property of the Instituto Superior Tecnico, Lisbon, Portugal, see Fig 8. Implementation issues and results of tests carried out with the MAYA AUV are briefly discussed in Maurya et al. (2008). Prior to testing the path following algorithm on the $DELFIM_x$ ASV, simulations were done with a full nonlinear model of the vessel. The outer loop controller parameters were tuned based on the bandwidth of the linearized equations of motion of the vessel about $1m/s$; see Maurya et al. (2009) for the details. The results of the simulations are shown in figures 9 and 10 that show the tracking error e and desired and actual heading, respectively. Figure 11 shows the results obtained with the $DELFIM_x$ ASV in the Azores, performing a lawn mowing maneuver during tests done in the scope of the European GREX project. Both in the simulations and in real tests the vehicle rejects the disturbance introduced by a fixed current. Furthermore, figure 11 shows that the performance of the path following algorithm is good even when the path contains arcs of circumferences.

CONCLUSIONS

This paper introduced an inner-outer control structure for marine vehicle path following in 2D, with due account for the vehicle dynamics and ocean currents. The structure is simple to implement and affords systems designers a convenient way of tuning the outer loop control law parameters as functions of a "bandwidth-like" characterization of the inner loop. Stability of the complete path following control system was proven for straight paths, by resorting to nonlinear control theoretical tools that borrow from input to output stability concepts and a related small gain theorem. The efficacy of the inner-outer control structure adopted was shown during tests with an AUV and an ASV at sea. Future work will aim at obtaining formal proofs of practical stability and convergence in the case of arbitrary spatial paths.

ACKNOWLEDGEMENTS

This work was supported in part by projects GREX/CEC-IST (EU contract No. 035223, http://www.grex-project.eu), Co3-AUVs (EU FP7 grant agreement No. 231378, http://www.Co3-AUVs.eu), and NAV-Control/FCT-PT (PTDC/EEA-ACR/65996/2006), the FREESUBNet RTN (EU contract number MRTN-CT-2006-036186, http://www.freesubnet.eu), and the FCT-ISR/IST plurianual funding and CMU-Portugal programs.

Fig. 7. The MAYA AUV

Fig. 8. The DELFIM$_x$ ASV

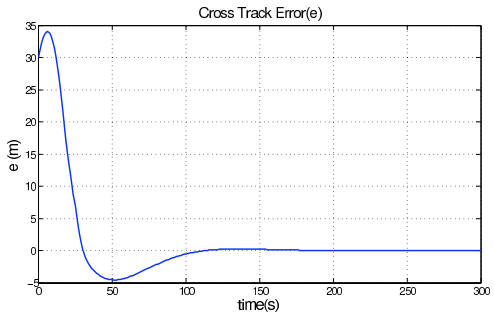

Fig. 9. Cross track error

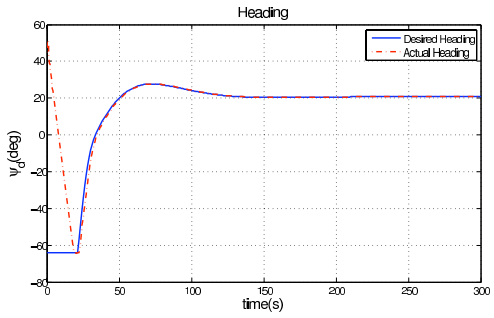

Fig. 10. Desired and actual heading

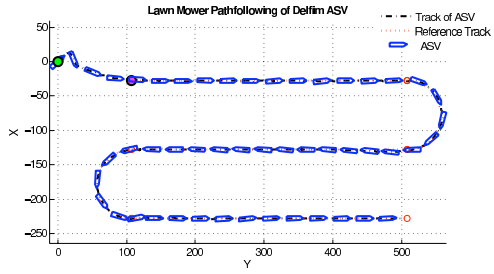

Fig. 11. Delfim$_x$ performing a lawn mowing maneuver in the Azores, PT

REFERENCES

Aguiar, A.P. and Hespanha, J. (2007). Trajectory-tracking and path-following of underactuated autonomous vehicles with parametric modeling uncertainty. *IEEE Transactions on Automatic Control*, 52(8), 1362–1379.

Aguiar, A.P., Hespanha, J., and Kokotovic, P. (2005). Path-following for non-minimum phase systems removes performance limitations. *IEEE Transactions on Automatic Control*, 50(2), 234–239.

Breivik, M. and Fossen, T. (2005). Principles of guidance-based path following in 2d and 3d. *44th IEEE Conference on Decision and Control, 2005 and 2005 European Control Conference. CDC-ECC '05.*, 627–634.

Encarnacao, P. and Pascoal, A. (2000). 3d path following for autonomous underwater vehicle. *Proceedings of the 39th IEEE Conference on Decision and Control, Sydney, Australia*, 3, 2977–2982.

Fossen, T. (2002). *Marine Control System: Guidance, Navigation and Control of Ships, Rigs and Underwater Vehicles*. Marine Cybernetics AS, Trondheim, Norway.

Ghabchello, R., Aguiar, A.P., Pascoal, A., Silvestre, C., Kaminer, I., and Hespanha, J. (2009). Coordinated path-following in the presence of communication losses and time delays. *SIAM J. Control Optim.*, 48(1), 234–265.

Indiveri, G. and Zizzari, A.A. (2008). Kinematics motion control of an underactuated vehicle: A 3d solution with bounded control effort. *Second IFAC Workshop on Navigation, Guidance and Control of Underwater Vehicles, Killaloe, Ireland.*

Khalil, H.K. (2001). *Nonlinear Systems (3rd Edition)*. Prentice Hall.

Maurya, P., Aguiar, A.P., and Pascoal, A. (2009). Marine vehicle path following using inner-outer loop control. *Technical Report , ISR/IST, Lisbon.*

Maurya, P., Navelkar, G., Madhan, R., Afzalpurkar, S., Prabhudesai, S., Desa, E., and Pascoal, A. (2008). Navigation and path following guidance of the maya auv: from concept to practice. *2nd International Conference on Underwater System Technology: Theory and Applications, Bali, Indonesia.*

Micaelli, A. and Samson, C. (1993). Trajectory-tracking for unicycle-type and two-steering-wheels mobile robots. In G. Roberts and R. Sutton (eds.), *Technical Report No. 2097, Project Icare, INRIA*, 353–386. Sophia-Antipolis, France.

Panteley, E. and Ortega, R. (1997). Cascaded control of feedback interconnected nonlinear systems: application to robots with ac drives. *Automatica*, 33(11), 1935–1947.

Park, S., Deyst, J., and How, J. (2007). Performance and lyapunov stability of a nonlinear path following guidance method. *Journal of Guidance, Control, and Dynamics*, 30(6), 1718–1728.

Pascoal, A., Silvestre, C., and Oliveira, P. (2006). Vehicle and mission control of single multiple autonomous marine robots. In G. Roberts and R. Sutton (eds.), *Advances in Unmanned Marine Vehicles*, 353–386. IEE Contol Engineering Series.

Silvestre, C. (2000). Multi-objective optimization theory with applications to the integrated design of controllers / plants for underwater vehicles. In *PhD Thesis*. Instituto Superior Técnico, Lisbon,Portugal.

Vanni, F. (2007). Coordinated motion control of multiple autonomous underwater vehicles. In *Masters Thesis*, 46–50. Instituto Superior Técnico, Lisbon,Portugal.